

Concentric Maclaurin spheroid models of rotating liquid planets

W. B. Hubbard

Lunar and Planetary Laboratory, University of Arizona, Tucson, AZ 85721

ABSTRACT

I present exact expressions for the interior gravitational potential V of a system of N concentric constant-density (Maclaurin) spheroids. I demonstrate an iteration procedure to find a self-consistent solution for the shapes of the interfaces between spheroids, and for the interior gravitational potential. The external free-space potential, expressed as a multipole expansion, emerges as part of the self-consistent solution. The procedure is both simpler and more precise than perturbation methods. One can choose the distribution and mass densities of the concentric spheroids so as to reproduce a prescribed barotrope to a specified accuracy. I demonstrate the method's efficacy by comparing its results with several published test cases.

Subject headings: Planets and satellites: interiors

1. Introduction

In its general form, the problem of the theory of figures is to find the external gravitational potential of a liquid planet in hydrostatic equilibrium, rotating at a uniform rate ω , and obeying a specified barotropic relationship for the dependence of pressure P on mass density ρ .

The expected precision (\sim one part in 10^9) of the *Juno* Jupiter orbiter spacecraft's measurements of Jupiter's gravity field will require a gravitational-modeling theory of unprecedented accuracy (Kaspi et al. 2010). Hubbard (2012) (Paper I) is an initial step toward such a theory. Paper I presents a new approach to the calculation of the multipole expansion of the external gravitational potential of a rotating planet in hydrostatic equilibrium.

As is well known, the problem of the theory of figures can be solved in closed or partially-closed form for a small number of special barotropes but arbitrary barotropes

generally require numerical methods. Analytic methods balloon in complexity even for the apparently simple case of two constant-density layers, the so-called two-layer Maclaurin spheroid (Schubert, Anderson, Zhang, Kong, & Helled 2011; Kong, Zhang, & Schubert 2012). In principle, such analytic complexity could be bypassed by seeking a purely numerical solution to the general equation of hydrostatic equilibrium. However, numerical solutions are vulnerable to numerical noise, produced for example by cancellation of nearly equal terms. In the traditional approach, cancellation of terms is mitigated by solving a hierarchy of integrodifferential equations generated from a perturbation expansion of the mass distribution in powers of the rotation rate (Zharkov & Trubitsyn 1978).

Paper I shows how the particular problem of the hydrostatic equilibrium of a rotating constant-density planet can be numerically solved to high precision by using gaussian quadrature to obtain the mass multipole moments. In this method, the moments are calculated by performing one-dimensional integrals over the surface mass distribution. Although gaussian quadrature is a numerical approximation to analytic integration, the results are exact (to within the floating point precision of the computer), as long as the integrand can be expressed as a polynomial of degree less than the degree of the gaussian quadrature; for a Maclaurin spheroid, using this approach with 48 quadrature points yields numerical results with a precision of at least $\sim 10^{-12}$. The mass multipole moments are then self-consistently iterated on the shape of the surface (Paper I). The method of Paper I largely bypasses the analytic complexity of perturbation methods and avoids cancellation problems, but as presented is only valid for a constant-density object, or for a constant-density object with special boundary conditions.

The present paper shows how the method of Paper I is straightforwardly generalized to solve the problem of multiple-layered constant-density spheroids. The resulting method, which I call the concentric Maclaurin spheroid (CMS) method, retains all of the advantages of the approach of Paper I, with the additional flexibility that the concentric Maclaurin spheroids can be arranged in sufficient numbers to closely approximate any prescribed barotrope. As we will see, an actual density discontinuity such as a discrete core or first-order phase transition is trivially incorporated in the CMS method, as opposed to the usual theories of figures.

In the following Section 2, I present the analytic development of the CMS method. In Section 3, I apply the CMS method to several published test cases and I show how the method can incorporate a prescribed barotrope. In the conclusion (Section 4), I discuss how the CMS method can be applied to analysis of *Juno* gravity data expected to arrive beginning in 2016.

2. Theory for N Layers of Maclaurin Spheroids

2.1. Exact calculation of gravitational potential

Consider a configuration of N concentric Maclaurin spheroids (Fig. 1). Label the spheroids with index $i = 0, 1, \dots, N - 1$, with $i = 0$ corresponding to the outermost spheroid and $i = N - 1$ corresponding to the innermost.

Because the gravitational potential V is linear in the mass density ρ , we may use the principle of superposition, such that the total potential at any point in space is the sum of the partial potentials of N concentric constant-density spheroids. Figure 2 illustrates this concept for a three-layer model.

Let the equatorial radius of the outermost spheroid be a_0 , and let the equatorial radii of the concentric spheroids be $a_0 > a_1 > a_2 > \dots > a_{N-1}$. The total external gravitational potential at some point "A" on the outermost level surface is

$$V_{\text{ext},A} = \frac{G}{r} \left(\sum_{k=0}^{\infty} D_{0,2k} r^{-2k} P_{2k}(\mu) + \sum_{k=0}^{\infty} D_{1,2k} r^{-2k} P_{2k}(\mu) + \dots + \sum_{k=0}^{\infty} D_{N-1,2k} r^{-2k} P_{2k}(\mu) \right), \quad (1)$$

where r is the radius from the center of the planet, μ is the cosine of the angle from the rotation axis, the $P_{2k}(\mu)$ are the usual Legendre polynomials,

$$D_{0,2k} = \frac{2\pi\rho_0}{2k+3} \int_{-1}^1 d\mu P_{2k}(\mu) r_0(\mu)^{2k+3}, \quad (2)$$

$$D_{1,2k} = \frac{2\pi(\rho_1 - \rho_0)}{2k+3} \int_{-1}^1 d\mu P_{2k}(\mu) r_1(\mu)^{2k+3}, \quad (3)$$

etc., where the relation $r_i = r_i(\mu)$ is the surface equipotential of the i -th layer. The zero-degree values are given by

$$D_{0,0} = \frac{2\pi\rho_0}{3} \int_{-1}^1 d\mu r_0(\mu)^3, \quad (4)$$

$$D_{i,0} = \frac{2\pi(\rho_i - \rho_{i-1})}{3} \int_{-1}^1 d\mu r_i(\mu)^3, \quad (5)$$

and so we have for the total mass M

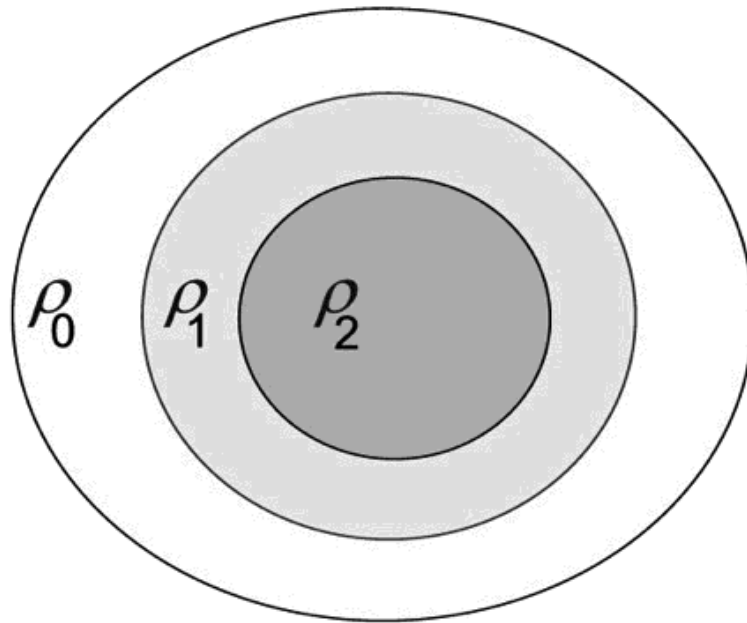


Fig. 1.— Concentric Maclaurin spheroids, each layer with constant density ρ , for the case $N = 3$.

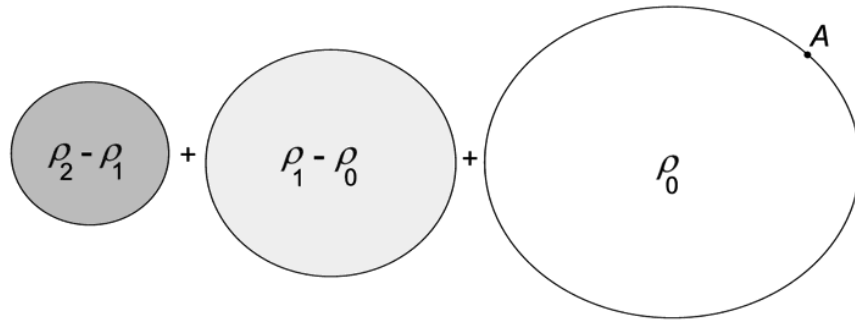


Fig. 2.— Method of superposition of Maclaurin spheroids, for the case $N = 3$. The point “A” is a typical point on the outermost surface of the planet.

$$M = \sum_{i=0}^{N-1} D_{i,0}. \quad (6)$$

We now introduce the usual dimensionless forms of the multipole moments,

$$M a_0^{2k} J_{i,2k} = -D_{i,2k}. \quad (7)$$

and the dimensionless radii of level surfaces

$$\xi_i = r_i(\mu)/a_0. \quad (8)$$

The total external gravitational potential at point “A” can thus be rewritten

$$V_{\text{ext},A} = \frac{GM}{r} \left(1 - \sum_{i=0}^{N-1} \sum_{k=1}^{\infty} J_{i,2k} \xi_0(\mu)^{-2k} P_{2k}(\mu) \right), \quad (9)$$

where

$$J_{i,2k} = - \left(\frac{3}{2k+3} \right) \left(\frac{\delta\rho_i \int_0^1 d\mu P_{2k}(\mu) \xi_i(\mu)^{2k+3}}{\sum_{j=0}^{N-1} \delta\rho_j \int_0^1 d\mu \xi_j(\mu)^3} \right), \quad (10)$$

$$\delta\rho_i = \rho_i - \rho_{i-1} \quad (11)$$

for $i > 0$ and

$$\delta\rho_0 = \rho_0. \quad (12)$$

Next, we must compute the total gravitational potential on an interior interface (level surface) at an arbitrary point “B”, as shown in Fig. 3.

First, we consider a problem in which there is only a mass distribution with a constant density $\delta\rho_i$ interior to point “B” located at coordinates (r, μ) . We calculate the external potential due to this mass distribution, finding

$$V_{i,\text{ext},B} = \frac{G}{r} \sum_{k=0}^{\infty} D_{i,2k} r^{-2k} P_{2k}(\mu). \quad (13)$$

Next we calculate the external potential at the surface of a spherical mass distribution with radius r and constant density $\delta\rho_{i-1}$ (shown as a dashed circle in Fig. 3):

$$V''_{i,\text{ext},B} = \frac{G}{r} \frac{4\pi\delta\rho_{i-1}}{3} r^3. \quad (14)$$

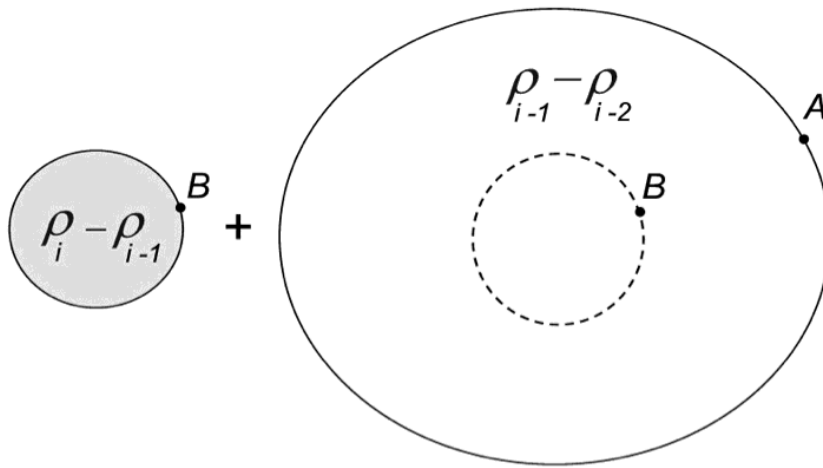


Fig. 3.— Schematic diagram illustrating the computation of three contributions to the gravitational potential at point “B” on an interior interface.

Finally, we calculate the internal potential at point “B” due to the mass distribution with constant density $\delta\rho_{i-1}$ external to the dashed circle in Fig. 3:

$$V'_{i,\text{int},B} = \frac{2\pi G}{r} \delta\rho_{i-1} \sum_{k=0}^{\infty} P_{2k}(\mu) \int_{-1}^1 d\mu' P_{2k}(\mu') \int_r^{r_{i-1}(\mu')} dr' r'^{-2k+1}. \quad (15)$$

Adding all contributions to the potential at point “B” due to the mass density in the i -th layer and in the $i-1$ -th layer, one has

$$V_{i,B} = \frac{G}{r} \sum_{k=0}^{\infty} D_{i,2k} r^{-2k} P_{2k}(\mu) + G \sum_{k=0}^{\infty} D'_{i-1,2k} r^{2k} P_{2k}(\mu) + G D''_{i-1,0} r^2, \quad (16)$$

where [cf Eq. (4)]

$$D_{i,2k} = \frac{4\pi\delta\rho_i}{2k+3} \int_0^1 d\mu P_{2k}(\mu) r_i(\mu)^{2k+3}, \quad (17)$$

for $k > 1$ we have

$$D'_{i-1,2k} = \frac{4\pi\delta\rho_{i-1}}{2-2k} \int_0^1 d\mu P_{2k}(\mu) r_{i-1}(\mu)^{2-2k}, \quad (18)$$

for $k = 1$ we have

$$D'_{i-1,2} = 4\pi\delta\rho_{i-1} \int_0^1 d\mu P_2(\mu) \ln[r_{i-1}(\mu)], \quad (19)$$

and for $k = 0$

$$D'_{i-1,0} = 2\pi\delta\rho_{i-1} \int_0^1 d\mu r_{i-1}(\mu)^2, \quad (20)$$

$$D''_{i-1,0} = -\frac{2\pi\delta\rho_{i-1}}{3}. \quad (21)$$

Next, analogous to Eq. (7), we introduce dimensionless forms of the $D'_{i-1,2k}$:

$$M a_0^{-1-2k} J'_{i,2k} = -D'_{i,2k}, \quad (22)$$

and

$$J''_{i,0} = \frac{2\pi\delta\rho_i a_0^3}{3M}. \quad (23)$$

By analogy with Eq. (10), we may write the dimensionless forms of Eqs. (18-21): for $k > 1$

$$J'_{i,2k} = -\left(\frac{3}{2-2k}\right) \left(\frac{\delta\rho_i \int_0^1 d\mu P_{2k}(\mu) \xi_i(\mu)^{2-2k}}{\sum_{j=0}^{N-1} \delta\rho_j \int_0^1 d\mu \xi_j(\mu)^3}\right), \quad (24)$$

for $k = 1$

$$J'_{i,2} = -3 \left(\frac{\delta\rho_i \int_0^1 d\mu P_2(\mu) \ln[\xi_i(\mu)]}{\sum_{j=0}^{N-1} \delta\rho_j \int_0^1 d\mu \xi_j(\mu)^3}\right), \quad (25)$$

and for $k = 0$

$$J'_{i,0} = - \left(\frac{3}{2} \right) \left(\frac{\delta\rho_i \int_0^1 d\mu P_{2k}(\mu) \xi_i(\mu)^2}{\sum_{j=0}^{N-1} \delta\rho_j \int_0^1 d\mu \xi_j(\mu)^3} \right), \quad (26)$$

$$J''_{i,0} = \frac{\delta\rho_i}{2 \sum_{j=0}^{N-1} \delta\rho_j \int_0^1 d\mu \xi_j(\mu)^3}. \quad (27)$$

Eq. (16) then takes the form

$$V_{i,B} = -\frac{GM}{a_0} \frac{1}{\xi} \left[\sum_{k=0}^{\infty} J_{i,2k} \xi^{-2k} P_{2k}(\mu) + \sum_{k=0}^{\infty} J'_{i-1,2k} \xi^{2k+1} P_{2k}(\mu) + J''_{i-1,0} \xi^3 \right]. \quad (28)$$

The total potential at a point B located at coordinates (ξ, μ) on the j -th interface is obtained by summing over all layers:

$$V_B(j) = -\frac{GM}{a_0} \frac{1}{\xi} \left[\sum_{i=j}^{N-1} \sum_{k=0}^{\infty} J_{i,2k} \xi^{-2k} P_{2k}(\mu) + \sum_{i=0}^{j-1} \sum_{k=0}^{\infty} J'_{i-1,2k} \xi^{2k+1} P_{2k}(\mu) + \sum_{i=0}^{j-1} J''_{i-1,0} \xi^3 \right]. \quad (29)$$

2.2. Parameters and scaling

Assume that the planet rotates as a solid body at an angular rate ω . Therefore in the corotating frame there appears a rotational potential

$$Q = \frac{1}{3} r^2 \omega^2 [1 - P_2(\mu)], \quad (30)$$

and the total potential U appearing in the equation of hydrostatic equilibrium

$$\nabla P = \rho \nabla U \quad (31)$$

is given by

$$U = V + Q. \quad (32)$$

For a nonrotating planet, all multipole moments for $k > 0$ vanish and the potential V within the planet depends only on r . The presence of the nonspherical term Q in U breaks the spherical symmetry and excites all of the $k > 0$ terms. We represent the magnitude of Q by the dimensionless parameter

$$q = \frac{\omega^2 a_0^3}{GM}. \quad (33)$$

The number and location of the concentric Maclaurin spheroids can be chosen arbitrarily. Let the equatorial radius of the i -th spheroid be a_i . Let

$$\lambda_i = \frac{a_i}{a_0}, i = 0, 1, \dots, N - 1. \quad (34)$$

The λ_i can be spaced equally between 0 and 1, or could be made denser in certain regions (for example, one could space them at two or three per density scale height).

Define the mean density of the planet:

$$\bar{\rho} = \frac{3M}{4\pi a_0^3} \frac{1}{\int_0^1 d\mu \xi_0(\mu)^3}. \quad (35)$$

For numerical convenience one may use the dimensionless density increment for the i -th spheroid:

$$\delta_i \equiv \delta\rho_i/\bar{\rho} \quad (36)$$

As can be seen by examining Eqs. (10, 24-27), the dimensionless multipole moments can be calculated using either the $\delta\rho_i$ or the δ_i . However, although the moments are dimensionless, further scaling is necessary in order to achieve satisfactory numerical accuracy. Consider, for example, a model with $N = 128$, having spheroids with equally-spaced equatorial radii. It then becomes necessary to consider spheroids with $\lambda_i \sim 1/100$, so for example $J'_{100,20}$ has an integrand $\sim 10^{-2 \times (-18)}$. The resulting huge number is then multiplied by $\sim 10^{-2 \times (+21)}$ in the corresponding term in Eq. (28). To avoid pointlessly multiplying and then dividing by large factors, we rescale to new variables and parameters:

$$\zeta_i(\mu) \equiv \xi_i(\mu)/\lambda_i, \quad (37)$$

$$\tilde{J}_{i,2k} \equiv J_{i,2k}/\lambda_i^{2k}, \quad (38)$$

$$\tilde{J}'_{i,2k} \equiv J'_{i,2k}\lambda_i^{2k+1}, \quad (39)$$

Then

$$\tilde{J}_{i,2k} = - \left(\frac{3}{2k+3} \right) \left(\frac{\delta_i \lambda_i^3 \int_0^1 d\mu P_{2k}(\mu) \zeta_i(\mu)^{2k+3}}{\sum_{j=0}^{N-1} \delta_j \lambda_j^3 \int_0^1 d\mu \zeta_j(\mu)^3} \right); \quad (40)$$

for $k > 1$

$$\tilde{J}'_{i,2k} = - \left(\frac{3}{2-2k} \right) \left(\frac{\delta_i \lambda_i^3 \int_0^1 d\mu P_{2k}(\mu) \zeta_i(\mu)^{2-2k}}{\sum_{j=0}^{N-1} \delta_j \lambda_j^3 \int_0^1 d\mu \zeta_j(\mu)^3} \right), \quad (41)$$

for $k = 1$

$$\tilde{J}'_{i,2} = -3 \left(\frac{\delta_i \lambda_i^3 \int_0^1 d\mu P_2(\mu) \ln[\zeta_i(\mu)]}{\sum_{j=0}^{N-1} \delta_j \lambda_j^3 \int_0^1 d\mu \zeta_j(\mu)^3} \right), \quad (42)$$

and for $k = 0$

$$\tilde{J}'_{i,0} = -\frac{3}{2} \left(\frac{\delta_i \lambda_i^3 \int_0^1 d\mu P_{2k}(\mu) \zeta_i(\mu)^2}{\sum_{j=0}^{N-1} \delta_j \lambda_j^3 \int_0^1 d\mu \zeta_j(\mu)^3} \right), \quad (43)$$

We introduce dimensionless planetary units of pressure (P_{pu}), density (ρ_{pu}), and total potential (U_{pu}), such that

$$P \equiv \frac{GM^2}{a_0^4} P_{\text{pu}}, \quad (44)$$

$$\rho \equiv \frac{M}{a_0^3} \rho_{\text{pu}}, \quad (45)$$

$$U \equiv \frac{GM}{a_0} U_{\text{pu}}. \quad (46)$$

Evaluating the total potential at the surface of the outermost Maclaurin spheroid at the equator ($\mu = 0$), we have

$$U_{0,\text{pu}} = 1 + \frac{1}{2}q - \sum_{i=0}^{N-1} \sum_{k=1}^{\infty} \tilde{J}_{i,2k} \lambda_i^{2k} P_{2k}(0). \quad (47)$$

At the surface of each subsequent Maclaurin spheroid we have

$$\begin{aligned} U_{j,\text{pu}} = & -\frac{1}{\lambda_j} \left(\sum_{i=j}^{N-1} \sum_{k=0}^{\infty} \tilde{J}_{i,2k} (\lambda_i/\lambda_j)^{2k} P_{2k}(0) \right. \\ & \left. + \sum_{i=0}^{j-1} \sum_{k=0}^{\infty} \tilde{J}'_{i,2k} (\lambda_j/\lambda_i)^{2k+1} P_{2k}(0) + \sum_{i=0}^{j-1} J''_{i,0} \lambda_j^3 \right) + \frac{1}{2}q \lambda_j^2. \end{aligned} \quad (48)$$

and at the center of the planet

$$U_{\text{center,pu}} = - \sum_{i=0}^{N-1} \tilde{J}'_{i,2k} \lambda_i = - \sum_{i=0}^{N-1} J'_{i,2k}. \quad (49)$$

The shape $\zeta_0(\mu)$ of the surface of the planet is an equipotential given by the solution to

$$\frac{1}{\zeta_0} \left(1 - \sum_{i=0}^{N-1} \sum_{k=1}^{\infty} \tilde{J}_{i,2k} \lambda_i^{2k} \zeta_0^{-2k} P_{2k}(\mu) \right) + \frac{1}{3} q \zeta_0^2 [1 - P_2(\mu)] = U_{0,\text{pu}}. \quad (50)$$

Correspondingly, the shape $\zeta_j(\mu)$ of the surface of the j -th spheroid is an equipotential given by the solution to

$$\begin{aligned} & -\frac{1}{\zeta_j} \left(\sum_{i=j}^{N-1} \sum_{k=0}^{\infty} \tilde{J}_{i,2k} (\lambda_i/\lambda_j)^{2k} \zeta_j^{-2k} P_{2k}(\mu) + \sum_{i=0}^{j-1} \sum_{k=0}^{\infty} \tilde{J}'_{i,2k} (\lambda_j/\lambda_i)^{2k+1} \zeta_j^{2k+1} P_{2k}(\mu) \right. \\ & \left. + \sum_{i=0}^{j-1} J''_{i,0} \lambda_j^3 \zeta_j^3 \right) + \frac{1}{3} q \lambda_j^3 \zeta_j^2 [1 - P_2(\mu)] + \left(\sum_{i=j}^{N-1} \sum_{k=0}^{\infty} \tilde{J}_{i,2k} (\lambda_i/\lambda_j)^{2k} P_{2k}(0) \right. \\ & \left. + \sum_{i=0}^{j-1} \sum_{k=0}^{\infty} \tilde{J}'_{i,2k} (\lambda_j/\lambda_i)^{2k+1} P_{2k}(0) + \sum_{i=0}^{j-1} J''_{i,0} \lambda_j^3 \right) - \frac{1}{2} q \lambda_j^3 = 0. \end{aligned} \quad (51)$$

2.3. Gaussian quadrature

All of the foregoing expressions for the potential of N concentric Maclaurin spheroids are exact. For practical applications, we are interested in finding the potential as a multipole expansion to finite (say, thirtieth) degree, corresponding to an upper limit at, say, $k_{\text{max}} = 15$. For this purpose one may numerically evaluate the angular integrals for the multipole moments using $L > 2k_{\text{max}}$ gaussian quadrature points. For the examples presented in this paper, we use $L = 48$ gaussian quadrature points μ_α , $\alpha = 1, 2, \dots, L$ with corresponding weights w_α , $\alpha = 1, 2, \dots, L$ over the interval $0 < \mu < 1$.

Using initial guesses for the moments $\tilde{J}_{i,2k}$, $\tilde{J}'_{i,2k}$, and $J''_{i,0}$, one solves Eqns. (50) and (51) for $\zeta_i(\mu_\alpha)$ for $i = 0, 1, \dots, N-1$ and $\alpha = 1, 2, \dots, L$. The solutions for these values are then used to evaluate the gravitational moments by gaussian quadrature,

$$\tilde{J}_{i,2k} \approx - \left(\frac{3}{2k+3} \right) \left(\frac{\delta_i \lambda_i^3 \sum_{\alpha=1}^L w_\alpha P_{2k}(\mu_\alpha) \zeta_i(\mu_\alpha)^{2k+3}}{\sum_{j=0}^{N-1} \delta_j \lambda_j^3 \sum_{\alpha=1}^L w_\alpha \zeta_j(\mu_\alpha)^3} \right), \quad (52)$$

etc.

One then iterates between calculation of the level surface shapes via Eqns. (50) and (51) and the gravitational moments via Eqns. (40-43) until the difference between successive

iterations falls below a specified tolerance. For the purposes of achieving *Juno*-level precision, about 30 such iterations (over all N spheroids) usually suffices.

2.4. Calculation of the barotrope

First, we calculate the density in each uniform layer; for the j -th layer

$$\rho_{j,\text{pu}} = \frac{\sum_{i=0}^j \delta_i}{\sum_{k=0}^{N-1} \delta_k \lambda_k^3 \sum_{\alpha=1}^L \zeta_k(\mu_\alpha)^3}. \quad (53)$$

Next, we calculate the total potential U_{pu} on the outer surface, on each of the interfaces, and at the center, using Eqs. (47-49). Since the density is constant between interfaces, Eq. (31) is trivially integrated to obtain the pressure at the bottom of the j -th layer:

$$P_{j,\text{pu}} = P_{j-1,\text{pu}} + \rho_{j-1,\text{pu}}(U_{j,\text{pu}} - U_{j-1,\text{pu}}). \quad (54)$$

Figure 4 shows an example of the resulting stair-step barotrope obtained for a rotating Jupiter model with $N = 32$ and a linear variation of density with mean radius (the linear-density model is discussed further below).

3. Comparison of CMS results with test cases

3.1. Linear density profile

Results for a linear density model of Jupiter using a fifth-order theory are tabulated in Table 3.1 of Zharkov & Trubitsyn (1978). They adopt a mass-density profile which is linear in the mean radius of a level surface rather than in its equatorial radius. The mean radius s_j of the j -th level surface relative to the planetary mean radius is given by

$$\frac{s_j}{s_0} = \left(\frac{\int_0^1 d\mu \xi_j(\mu)^3}{\int_0^1 d\mu \xi_0(\mu)^3} \right)^{1/3}. \quad (55)$$

If we arrange a constant increment δ_j in λ_j (with constant $\Delta\lambda$), we can make the resulting density linear in s/s_0 by modifying the density increment for each spheroid to

$$\delta_{j,s} = \delta_j \frac{\Delta s}{\Delta \lambda}. \quad (56)$$

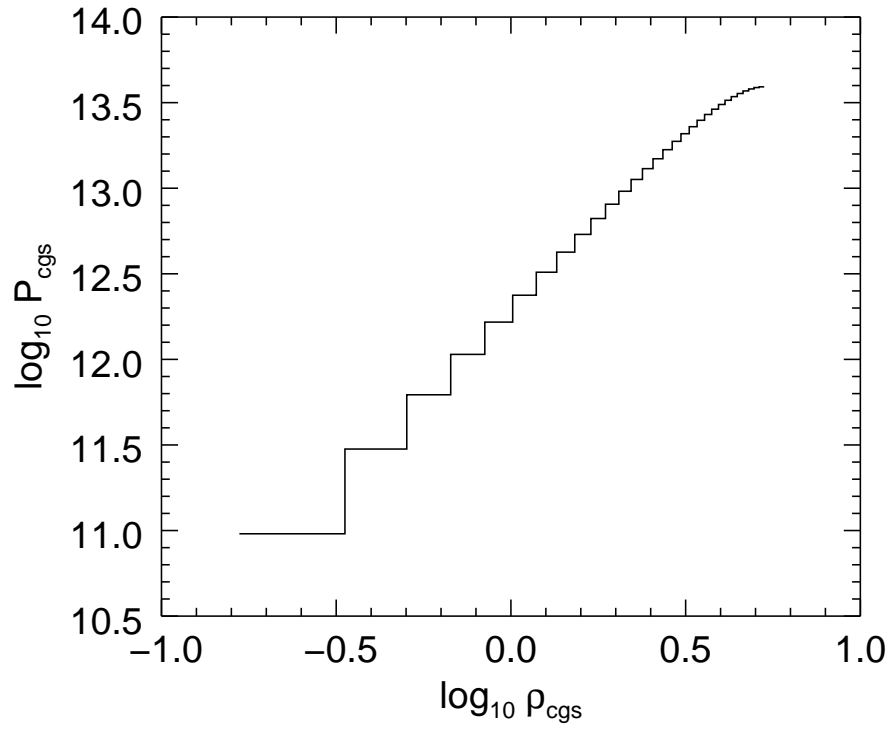


Fig. 4.— Inferred variation of pressure vs. density (both in c.g.s. units) in a CMS model of Jupiter with $N = 32$, for an assumed linear variation of mass density with mean radius.

The intervals Δs must be computed iteratively. Furthermore, Zharkov & Trubitsyn (1978) expand their fifth-order theory in powers of the small parameter

$$m = \frac{\omega^2 s_0^3}{GM}, \quad (57)$$

with a fixed value of m that differs slightly from the value obtained from the value obtained for a more realistic Jupiter model. Thus, the CMS calculations must be also iterated to obtain a value for m that matches the one given by Zharkov & Trubitsyn (1978).

Table 1 presents a comparison of results for the linear-density model. Agreement is excellent for $N = 128$. The inferred pressure-density relation for $N = 32$ was depicted in Fig. 4.

3.2. Two-layer Maclaurin spheroids

The relative simplicity and elegance of Maclaurin’s theory for the single spheroid disappears for $N = 2$. Nevertheless, one finds considerable literature for the case $N = 2$, dating back at least to Darwin (1903).

First, it is useful to test the CMS theory by calculating the equipotential shape of an interior interface in a Maclaurin spheroid of uniform density. For this test, I set $N = 2$, $\lambda_1 = 0.5$, $\delta_0 = 1$, $\delta_1 = 0$. I set q equal to the Jovian value adopted in Paper I. The converged CMS model agrees exactly with results presented in Paper I, as it should. Figure 5 shows the deviations of the outer and intermediate surfaces from ellipsoids of revolution, with $\delta\zeta = \zeta(\mu) - 1/\sqrt{(1 + \ell^2\mu^2)}$, where ℓ is related to m by Maclaurin’s result, $m = \frac{3}{2\ell^3}[(3 + \ell^2)\arctan \ell - 3\ell]$. Evidently the shape of the intermediate surface is to high precision an ellipsoid of revolution, homologous to the outer surface, as it is in Maclaurin’s analytic theory.

Next, I compare my $N = 2$ CMS results with the results of Schubert, Anderson, Zhang, Kong, & Helled (2011). The Schubert et al. models are characterized by three parameters,

$$Q_v = \frac{\int_0^1 d\mu \xi_1(\mu)^3}{\int_0^1 d\mu \xi_0(\mu)^3}, \quad (58)$$

the core-envelope density ratio ρ_1/ρ_0 , and a dimensionless rotation parameter

$$\epsilon_2 = \frac{\omega^2}{2\pi G\rho_0}, \quad (59)$$

all in my notation. In the present paper I compare three models adopted by Schubert, Anderson, Zhang, Kong, & Helled (2011): “Mars”, “Neptune”, and “Uranus2”. The quantities that they compute for these

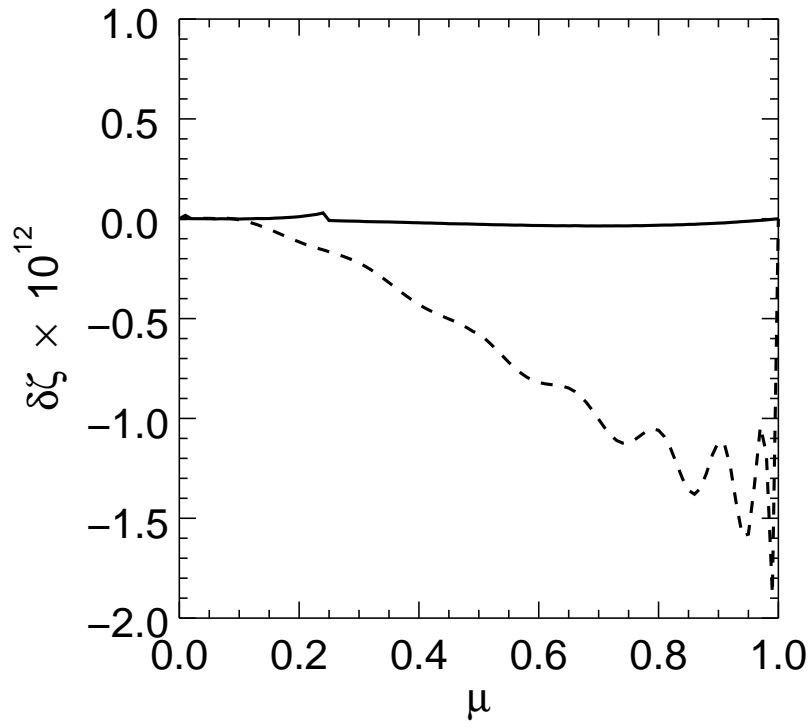


Fig. 5.— Departure of outer surface (dashed) and intermediate surface (solid) from an ellipsoid of revolution, for a classical Maclaurin spheroid.

models are J_2 , and E_0 and E_1 , respectively the eccentricities of the outer surface and intermediate surface, defined by

$$E = \sqrt{1 - (1 - e)^2}, \quad (60)$$

where the oblateness $e = 1 - \zeta(\mu = 1)$. The CMS calculations require iteration to match the values of Q_v and ϵ_2 . Results are presented in Tables 2-4. While the values for “Mars” generally agree, there are unexplained discrepancies for “Neptune” and “Uranus2”. The “3rd order” results of Schubert et al. agree with CMS results to high precision, but their “exact” results differ by larger-than-expected amounts.

3.3. Polytrope of index one

The polytrope of index one is defined by the barotrope

$$P = K\rho^2, \quad (61)$$

where the polytropic constant K is chosen in the present application to yield a model planet matched to Jupiter’s mass and equatorial radius. Rotating planet models obeying this barotrope have been extensively studied (Zharkov & Trubitsyn 1978; Hubbard 1975), so it provides a rigorous test of the CMS method.

Moreover, the study presented in this section provides a useful illustration of how, for a chosen barotrope, one may choose CMS arrays of λ_j and δ_j to yield a close match to the barotrope.

For a nonrotating $n = 1$ polytrope, the density distribution is given by

$$\rho = \rho_c \frac{\sin \pi \lambda}{\pi \lambda}, \quad (62)$$

where ρ_c is the central density. To obtain a first approximation to the δ distribution over the spheroids, we differentiate:

$$\frac{d(\rho/\rho_c)}{d\lambda} = \frac{\cos \pi \lambda}{\lambda} - \frac{\sin \pi \lambda}{\pi \lambda^2}, \quad (63)$$

and we use this relation to obtain starting values of the δ_j .

After obtaining a converged hydrostatic-equilibrium model for N spheroids with the above array of δ_j , one calculates the arrays $U_{j,\text{pu}}$ and $P_{j,\text{pu}}$. Next one calculates an array of desired densities $\rho_{j,\text{pu,desired}}$ according to

$$\rho_{j,\text{pu,desired}} = \rho \left(\frac{1}{2} (P_{j+1} + P_j) \right), \quad (64)$$

where $\rho(P)$ is the inverse of the adopted barotrope $P(\rho)$. Differencing the desired densities between layers then gives a new array of δ_j . In general, it is necessary to scale the densities so as to obtain the correct total mass of the CMS model. This can be effected by rewriting the barotrope as

$$P = P(C\rho), \quad (65)$$

where C is a dimensionless factor. For the polytrope of index one, when one adopts a value of C greater or less than one, this is equivalent to redefining the value of K .

After obtaining a new converged CMS model, the process of adjusting the densities to obtain a new array of $\rho_{j,\text{pu,desired}}$, etc., continues until all changes in gravitational moments and in the value of C are reduced to within a specified tolerance. Because of the additional step of fitting the barotrope, more iterations are required for convergence. Figure 6 shows the fitted and target $n = 1$ barotrope of a converged 512-layer CMS model of Jupiter.

The comparison models for the $n = 1$ polytrope are (1) analytic expansions of J_2 , J_4 , and J_6 to order q^3 (Zharkov & Trubitsyn 1978; Hubbard 1975), and (2) a self-consistent-field calculation of the rotating polytrope based on the analytic result that the interior density can be expanded as a series of products of spherical harmonics and spherical Bessel functions j_n (Hubbard 1975). Table 6 presents results for $N = 256$ and $N = 512$ CMS models along with the comparison models. The results for J_2 for the $N = 512$ CMS model were still changing in the fifth figure after the decimal point after fifteen iterations on the barotrope fit.

3.4. Convergence considerations

Kong, Zhang, & Schubert (2013) have criticized the Maclaurin spheroid approach employed in this paper, stating that the method of Paper I is incomplete. Further clarification is called for since the method of Paper I is central to the CMS method.

Consider a Maclaurin spheroid of eccentricity ℓ . For its external potential write, as usual,

$$V_{\text{ext}}(r, \mu) = \frac{GM}{r} \left[1 - \sum_{k=1}^{\infty} \left(\frac{a}{r}\right)^{2k} J_{2k} P_{2k}(\mu) \right]. \quad (66)$$

Where does this infinite-series expansion diverge for the Maclaurin spheroid? Evaluate it at the spheroid's pole, where $\mu = 1$ and $r^2/a^2 = b^2/a^2 = 1/(1 + \ell^2)$. Substitute Eq. (10) of Hubbard (2012). We get

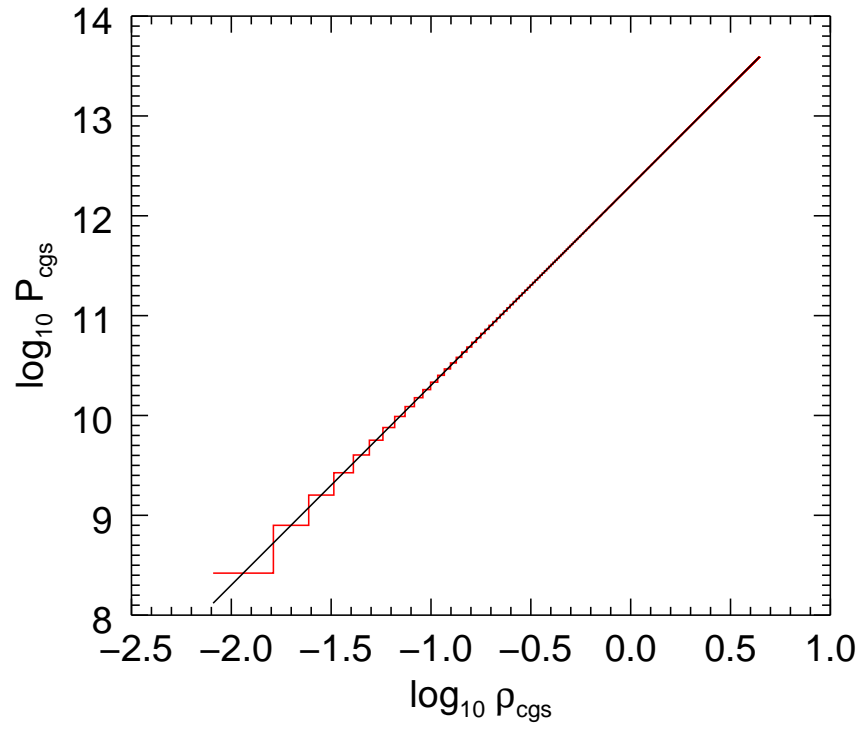


Fig. 6.— Target (solid line) $n = 1$ barotrope for a Jupiter model, and fitted $N = 512$ CMS barotrope (stairstep).

$$V(b, 1) = \frac{GM}{b} \left[1 - \sum_{k=1}^{\infty} \frac{3(-1)^{1+k} \ell^{2k}}{(2k+1)(2k+3)} \right]. \quad (67)$$

The ratio of the $k + 1$ -th to the k -th term is

$$\frac{t_{k+1}}{t_k} = -\ell^2 \frac{(2k+1)(2k+3)}{(2k+3)(2k+5)}. \quad (68)$$

Therefore the series converges if $\ell^2 < 1$ or the oblateness $e < 1 - b/a = 1 - 1/\sqrt{2} = 0.29289$, in agreement with the estimate of Kong, Zhang, & Schubert (2013). The corresponding $m = m_{\text{crit}} = 0.212389$ and $q = q_{\text{crit}} = 0.424778$. These values are far larger than the parameters of any known planet. Note, by the way, that the point of bifurcation for the Maclaurin-Jacobi ellipsoid sequence is at a somewhat larger $\ell_{\text{bifurc}} = 1.39$, corresponding to $m_{\text{bifurc}} = 0.280$ and $q_{\text{bifurc}} = 0.669$.

Paper I shows that for a Maclaurin spheroid with Jupiter’s $q = 0.089$, my method gives for the shape of the spheroid’s surface a numerical result that differs no more than a few parts in 10^{13} from the exact Maclaurin shape. Note that Figure 5 of this paper shows similarly-small departures at the outer surface and on an intermediate surface. Thus, for this value of q , any neglected terms in Equation (66) will not exceed $\sim 10^{-12}$ of the included terms.

Repeating the calculation for a Maclaurin spheroid with a Saturn-like $q = 0.155$, I obtain results shown in Figure 7 for the relative difference of the spheroid’s surface radius from the exact Maclaurin ellipsoid shape. The departures are, in absolute terms, no more than a few centimeters, and would have no significance whatsoever for practical models of Saturn’s gravity field. Moreover, the real Saturn is much less oblate than the Maclaurin model, so the departures of a CMS model from an “exact” model will be smaller still.

As in Paper I, the general CMS method relies upon the requirement that the external multipole expansion (66) of a given spheroid’s potential converges at all points on the spheroid’s surface. First, on a sphere of radius $r = a_0$, the expansion converges. To see this, note that $J_{2k} \sim (-1)^{k+1} q^k$ for a uniformly-rotating body in hydrostatic equilibrium. Thus, on the sphere $\xi_0 = 1$, the ratio of the $k + 1$ -th term to the k -th term is $\sim -q$, so for $q < 1$ the series converges.

Next we examine the series convergence at the pole, $\mu = 1$, where $\xi_0 = 1 - e$, where $e \sim q$ is the oblateness. At $\mu = 1$, the ratio of the $k + 1$ -th term to the k -th term is $\sim -q/(1 - e)^2$. Thus, as long as $q < C'(1 - e)^2$ (where C' is a constant of order unity

whose precise value depends on the barotrope) the series converges. As discussed, the q values for Jupiter and Saturn are such that the convergence criterion is well satisfied (as numerically demonstrated for the test cases). See also a relevant discussion in Section 38 of Zharkov & Trubitsyn (1978).

4. Practical application to analysis of gravity data

The CMS analysis technique presented here can be vectorized for efficiency, although no significant effort has been made to do so at this point. For practical computations it will probably be necessary to further increase N and to increase the number of iterations on the barotrope fit, in order to match the theoretical results to the expected precision of spacecraft measurements.

Further iteration loops will be required if a subset of the calculated J_{2k} are to be fitted to observed values. Adjustable parameters might include: (1) the mass and density of a discrete core at the planet’s center, (2) chemical and density discontinuities at various layers, and (3) modifications to the assumed barotrope (crudely illustrated in this paper with the scale factor C).

As is obvious, there exists an infinity of possible arrangements of spheroids which can be fitted to a finite set of gravity data. Thus, a unique inversion cannot be achieved. However, application of specific physically-based barotropes and cosmochemical considerations can lead to the most realistic interior models.

5. Conclusion

One can further generalize the CMS method in two directions. First, in addition to the rotational potential Q one may introduce a tidal potential from a satellite. The resulting tidal perturbing potential Q_{tid} will be a function of two angular variables, μ and ϕ , where ϕ is the angle from the sub-satellite longitude. Since Q_{tid} will excite both zonal and tesseral gravity harmonics, evaluation of the response on all CMS surfaces will require two-dimensional rather than one-dimensional integrals. However, there appears to be no practical barrier to evaluating such integrals using two-dimensional gaussian quadrature (to be sure, at the cost of more computing time).

Second, one can investigate the effects of differential rotation on cylinders (for related investigations, see Kong, Zhang, & Schubert (2012) and Hubbard (1982)).

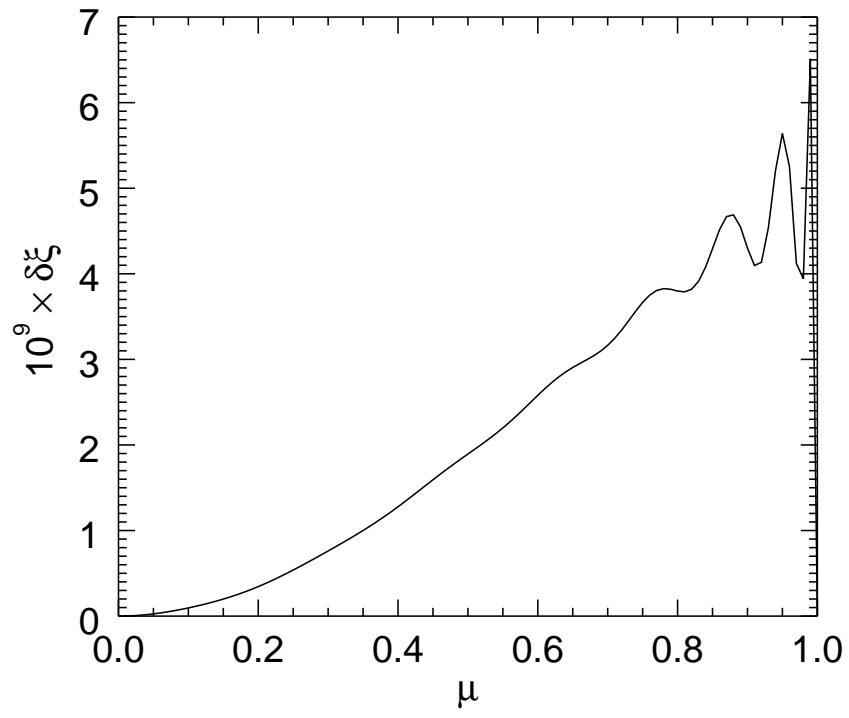


Fig. 7.— Calculation of the difference $\delta\xi = \xi_{\text{CMS}} - \xi_{\text{exact}}$ for a Maclaurin spheroid with Saturn’s mass, mean density, and rotation rate.

This research is supported by the *Juno* project under Subcontract 699053X from the Southwest Research Institute to the University of Arizona.

REFERENCES

- Darwin, G. H., 1903, *Trans. Am. Math. Soc.*, 4, 113
- Hubbard, W. B. 1975, *Sov. Astron. - AJ*, 18, 621
- Hubbard, W. B. 1982, *Icarus*, 52, 509
- Hubbard, W. B. 2012, *ApJ*, 756, L15.
- Kaspi, Y., Hubbard, W. B., Showman, A. P., & Flierl, G. R. 2010, *Geophys. Res. Lett.*, 37, L01204
- Kong, D., Zhang, K., & Schubert, G., 2012, *ApJ*, 748, 143
- Kong, D., Zhang, K., & Schubert, G., 2013, *ApJ*, 764, 67
- Schubert, G., Anderson, J., Zhang, K., Kong, D., & Helled, R., 2012, *Phys. Earth and Planetary Interiors*, 187, 364
- Zharkov, V. N., & Trubitsyn, V. P. 1978, *Physics of Planetary Interiors*, Tucson: Pachart

Table 1. Linear Density Model

Quantity	ZT ^a 5 th -order theory	CMS theory ($N = 128$)
q	...	0.088822426
m	0.0830	0.082999915
$J_2 \times 10^2$	1.4798	1.4798138
$-J_4 \times 10^4$	5.929	5.9269129
$J_6 \times 10^5$	3.497	3.4935680
$-J_8 \times 10^6$	2.52	2.5493209
$J_{10} \times 10^7$	2.4	2.1308951
$-J_{12} \times 10^8$...	1.9564143
$J_{14} \times 10^9$...	1.9237724

^aZharkov & Trubitsyn (1978)

Table 2. “Mars” **Note.** “3rd order” and “exact” values from Schubert et al. (2013)

Quantity	value	“3rd order”	“exact”	CMS ($N = 2$)
Q_v	0.125			
ρ_0/ρ_1	0.486			
ϵ_2	0.00347			
q	0.0046205430			
$J_2 \times 10^6$...	1823.18	1823.1	1823.1832
E_1	...	0.0888747	0.088859	0.088874693
E_0	...	0.100295	0.10030	0.10029471

Table 3. “Neptune” **Note.** “3rd order” and “exact” values from Schubert et al. (2013)

Quantity	value	“3rd order”	“exact”	CMS ($N = 2$)
Q_v	0.091125			
ρ_0/ρ_1	0.157334			
ϵ_2	0.0254179			
q	0.026207112			
$J_2 \times 10^6$...	6188.92	6241.0	6188.9267
E_1	...	0.143515	0.15147	0.14351534
E_0	...	0.209658	0.21019	0.20965898

Table 4. “Uranus2” **Note.** “3rd order” and “exact” values from Schubert et al. (2013)

Quantity	value	“3rd order”	“exact”	CMS ($N = 2$)
Q_v	0.0563272			
ρ_0/ρ_1	0.0791231			
ϵ_2	0.0318902			
q	0.029581022			
$J_2 \times 10^6$...	5680.32	5801.4	5680.3242
E_1	...	0.115655	0.14160	0.11565564
E_0	...	0.213648	0.21473	0.21364898

Table 5. Polytrope $n = 1$

Quantity	3rd order theory	j_n expansion	CMS ($N = 256$)	CMS ($N = 512$)
q	0.089195487	0.089195487	0.089195487	0.089195487
$J_2 \times 10^2$	1.3994099	1.3988511	1.3991574	1.3989253
$-J_4 \times 10^4$	5.3871087	5.3182810	5.3203374	5.3187997
$J_6 \times 10^5$	3.9972442	3.0118323	3.0133819	3.0122356
$-J_8 \times 10^6$...	2.1321157	2.1334136	2.1324628
$J_{10} \times 10^7$...	1.7406710	1.7418428	1.7409925
$-J_{12} \times 10^8$...	1.5682179	1.5693324	1.5685327
$J_{14} \times 10^9$...	1.5180877	1.5191923	1.5184156